

Supplementary Information

A tunable deep eutectic solvent platform for efficient and sustainable agarose extraction

Jie Luo^{a, b, c}, Simiao Di^{a, b, c}, Yongqiang Lian^{a, b, c}, Haijin Mou^a, Wen-Can Huang^{a, b, c*}

^a State Key Laboratory of Marine Food Processing and Safety Control, College of Food Science and Engineering, Ocean University of China, Qingdao 266404, China

^b Qingdao Key Laboratory of Green Manufacturing of Marine Bioproducts, Qingdao Institute of Marine Bio-manufacturing Industry, Qingdao 266071, China

^c Key Laboratory of Biological Processing of Aquatic Products, China National Light Industry, Qingdao 266404, China

Materials

N-Methylurea, disodium ethylenediaminetetraacetate (EDTA-Na₂), sodium hypochlorite, resorcinol, and dimethyl sulfoxide (DMSO) were purchased from Macklin Biochemical Co., Ltd. Benzyltriethylammonium chloride and 1,1-diethoxyethane were purchased from Aladdin Biochemical Technology Co., Ltd. Sodium hydroxide, concentrated hydrochloric acid, concentrated sulfuric acid, oxalic acid, potassium bromide, D-fructose, and ethanol were purchased from Sinopharm Chemical Reagent Co., Ltd. All reagents were of analytical grade and used without further purification unless otherwise specified.

Pretreatment of *Gelidium amansii*

Raw *Gelidium amansii* was soaked in water until fully softened, then thoroughly rinsed with clean water to remove impurities. The softened biomass was further washed with deionized water, followed by drying at 60 °C. The dried *Gelidium amansii* was ground using a mechanical grinder and passed through a 50-mesh sieve to obtain *Gelidium amansii* powder.

Quantum chemical calculations

Density functional theory (DFT) calculations were performed using the Gaussian 16. The geometry optimization and frequency analysis were conducted at the B3LYP-D3BJ/6-31G(d,p) level, while single-point energy calculations were performed at the B3LYP-D3BJ/6-311G(d,p) level. Electrostatic potential (ESP) mapping, reduced density gradient (RDG) analysis, and energy decomposition analysis based on force fields (EDA-FF) were conducted using the Multiwfn and VMD software packages. EDA-FF parameters were derived from the AMBER force field. In the three-molecule

system, carbon atoms were assigned as CA or CT; hydrogen atoms were typed as HA, HP, HC, H, or H1; oxygen atoms as O, OH, or OS; nitrogen atoms as N3 or NA; and chlorine atoms as IM.

Molecular dynamics simulation

Molecular structures of agarose, NMU, and TEBAC were constructed and initially optimized using Discovery Studio. Further geometry optimization of NMU and TEBAC was carried out at the B97-3c level using the ORCA 5.0 program, while agarose was optimized using the molecular mechanics module in Discovery Studio. Based on the optimized structures, restrained electrostatic potential (RESP) charges were fitted using Multiwfn, and topology files compatible with the GAFF2 force field were generated using Sobtop.

All-atom molecular dynamics simulations were performed using the GROMACS 2021. A cubic simulation box (10 nm × 10 nm × 10 nm) was constructed by randomly placing 1000 TEBAC molecules, 4000 NMU molecules, and 32 agarose molecules using Packmol. Subsequently, a 100 ps NVT (constant Number of particles, Volume, and Temperature) equilibration was carried out to raise the system temperature to the target value. This was followed by a 1000 ps NPT (constant Number of particles, Pressure, and Temperature) equilibration involving five rounds of annealing, in which the temperature was cycled between 600 K and 358 K to facilitate system equilibration

Production runs were performed for a total of 100.0 ns, using the leap-frog algorithm to integrate the Newtonian equations of motion with a time step of 0.002 ps over 50,000,000 steps. Temperature coupling was maintained using the V-rescale algorithm: the system was annealed from 600 K to 358.15 K over the first 20 ns, followed by a constant temperature phase at 358.15 K for the remaining 80 ns. Pressure

was controlled at 1.0 bar using the Parrinello-Rahman barostat. Long-range electrostatic interactions were treated with the particle-mesh Ewald (PME) method, and dispersion corrections were applied for van der Waals interactions due to the use of a cutoff scheme. Periodic boundary conditions were applied in all three spatial dimensions. Trajectory analysis was performed using GROMACS built-in tools, and molecular visualization was carried out using PyMOL.

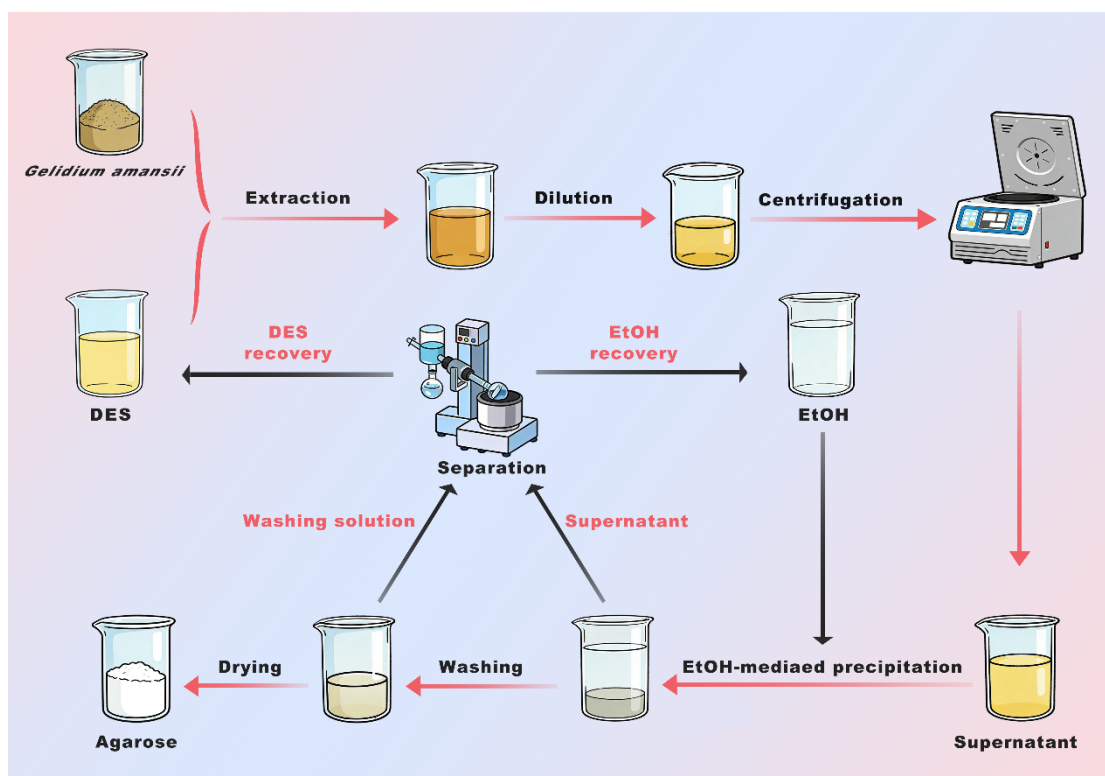


Fig. S1. Flowchart of agarose extraction using the DES method.

Results

Table S1. Physicochemical properties of the DES and its components.

Component	Viscosity (85°C, mPa·s)	Melting temperature (°C)
DES	49.25	-113.7
TEBAC	—	195.3
NMU	—	99.1

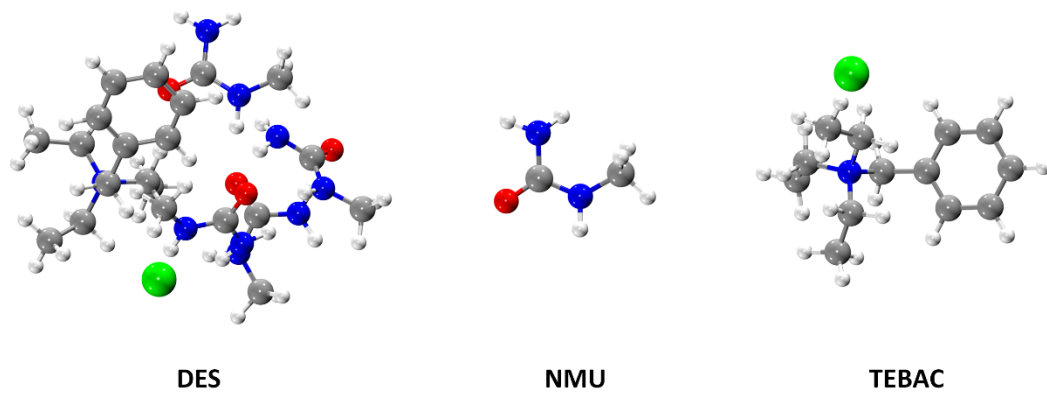


Fig. S2. Optimized geometry of the DES and its components.

Table S2. Energy, binding energy, and energy decomposition of TEBAC, NMU, and DES.

	Category	Energy value (a.u.)	Energy value (kcal/mol)
Energy decomposition	Electrostatic energy	—	-141.84
	Dispersion energy	—	-124.39
	Repulsion energy	—	117.71
	Total interaction energy	—	-148.52
Energy and binding energy of DES	TEBAC	-1023.8226	—
	NMU	-264.6655	—
	DES	-2082.6328	—
	Binding energy	-0.1481	-92.95

Notes: 1. Energy decomposition analyzes interactions between a TEBAC molecule and four NMU molecules. Total interaction energy = Electrostatic Energy + Dispersion Energy + Repulsion Energy.

2. Binding energy was calculated as $E_b = E(\text{DES}) - E(\text{TEBAC}) - 4E(\text{NMU})$, where $E(\text{DES})$ is the total energy of DES, $E(\text{TEBAC})$ is the energy of one TEBAC molecule, and $E(\text{NMU})$ is the energy of one NMU molecule.

Table S3. Physicochemical properties of agarose extracted by different methods.

Parameters	Alkali-EDTA	DES
Yield (%)	7.94 ± 0.53	16.50 ± 0.00
Gel strength (g/cm ²)	1447.20 ± 41.19	1107.50 ± 46.00
Sulfate content (%)	0.20 ± 0.02	0.36 ± 0.01
3,6-AG content (%)	47.95 ± 3.08	54.42 ± 2.46
Whiteness (%)	30.57 ± 2.31	29.79 ± 0.47
Transparency (%)	0.56 ± 0.02	0.70 ± 0.02
Melting temperature (°C)	88.70 ± 1.00	91.39 ± 1.66
Gelling temperature (°C)	32.80 ± 2.09	37.09 ± 1.35
Viscosity (80°C, mPa·s)	85.4 ± 1.3	63.2 ± 1.7

Table S4. Particle size and zeta potential of agarose extracted by different methods.

Parameters	Alkali-EDTA	DES
Size (nm)	452.1 ± 10.5	1145.7 ± 41.0
Zeta potential (mV)	-4.84 ± 0.12	-10.7 ± 0.26

Table S5. Energy, binding energy, and energy decomposition of agarose fragment and DES-agarose complex.

	Category	Energy value (a.u.)	Energy value (kcal/mol)
Energy decomposition	Electrostatic energy	—	-247.09
	Dispersion energy	—	-229.78
	Repulsion energy	—	196.92
	Total interaction energy	—	-279.95
Energy and binding energy of DES	Agarose	-2367.3546	—
	DES-agarose	-4450.0606	—
	Binding energy	-0.2213	-138.87

Notes: 1. Energy decomposition analyzes interactions between DES and agarose. Total interaction energy = Electrostatic energy + Dispersion energy + Repulsion energy.

2. Binding energy was calculated as $E_b = E(\text{DES-Agarose}) - E(\text{TEBAC}) - 4E(\text{NMU}) - E(\text{Agarose})$, where $E(\text{DES - Agarose})$ is the energy of the DES-Agarose complex, $E(\text{TEBAC})$ is the energy of one TEBAC molecule, $E(\text{NMU})$ is the energy of one NMU molecule, and $E(\text{Agarose})$ is the energy of agarose.

Cytocompatibility of DES-extracted agarose in L929 cells

L929 cells were seeded and cultured for 24 h before treatment with 100 μ L of DES-extracted agarose samples (n=3 per group) at various concentrations. Cells were incubated at 37 $^{\circ}$ C for 4 h, after which the medium was replaced with fresh medium containing 10 μ L CCK-8 reagent per well. Following 1 h incubation, absorbance at 450 nm was measured using a microplate reader, and cell viability was calculated as:

$$\text{Cell viability (\%)} = \frac{OD_{450a}}{OD_{450b}} \times 100\%$$

DES-extracted agarose exhibited high biocompatibility at 2.5 mg/mL, with L929 cell viability of 96.9%. Cell viability decreased in a concentration-dependent manner, reaching 84.2% and 83.7% at 5 and 10 mg/mL, respectively.

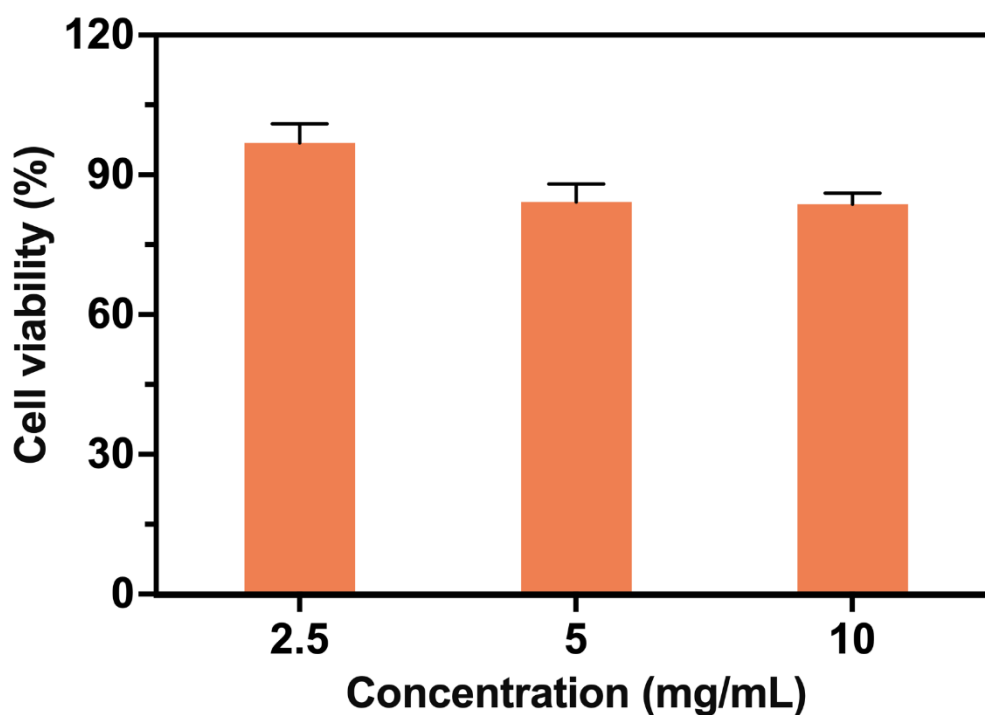


Fig. S3. Cytocompatibility of DES-extracted agarose.

Recycling Performance of DES in Agarose Extraction

After extraction, the supernatant from the alcohol precipitation step was collected and subjected to rotary evaporation at 40 °C for 1 h. The resulting alcohol and DES phases were separated, weighed, and the DES recovery yield calculated. Recovered DES, supplemented with a small amount of fresh DES, was reused for subsequent extraction cycles. DES was recovered with a recovery yield of 71.4% in a single cycle. When reused for three consecutive cycles with minor supplementation, both agarose yield and gel strength remained stable, showing no significant decline.

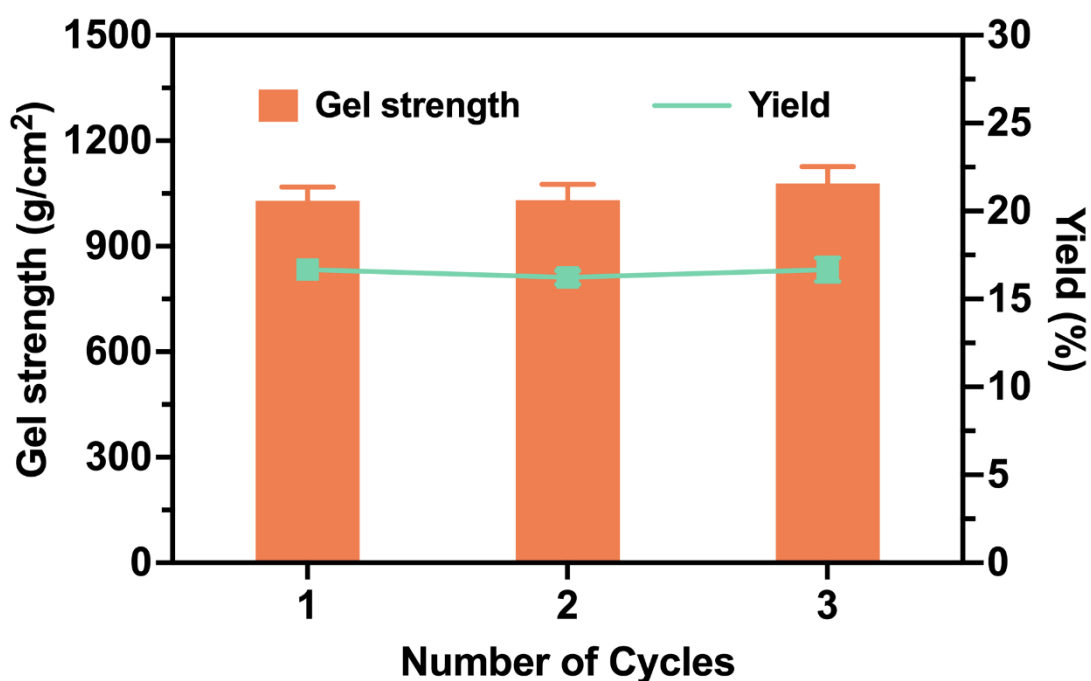


Fig. S4. Agarose yield and gel strength during three consecutive DES reuse cycles.

FTIR Analysis of Recovered DES after Three Reuse Cycles

The chemical structure and composition of DES after three reuse cycles were evaluated by FTIR spectroscopy. The spectra of recovered DES closely matched those of freshly prepared DES, with no noticeable shifts in the N–H stretching region (3500–3200 cm^{-1}), C=O stretching ($\sim 1650 \text{ cm}^{-1}$), C–H stretching (3000–2800 cm^{-1}), or the fingerprint region (1000–1500 cm^{-1}). These results indicate that the functional groups and overall chemical composition of the DES remained stable after repeated extraction cycles.

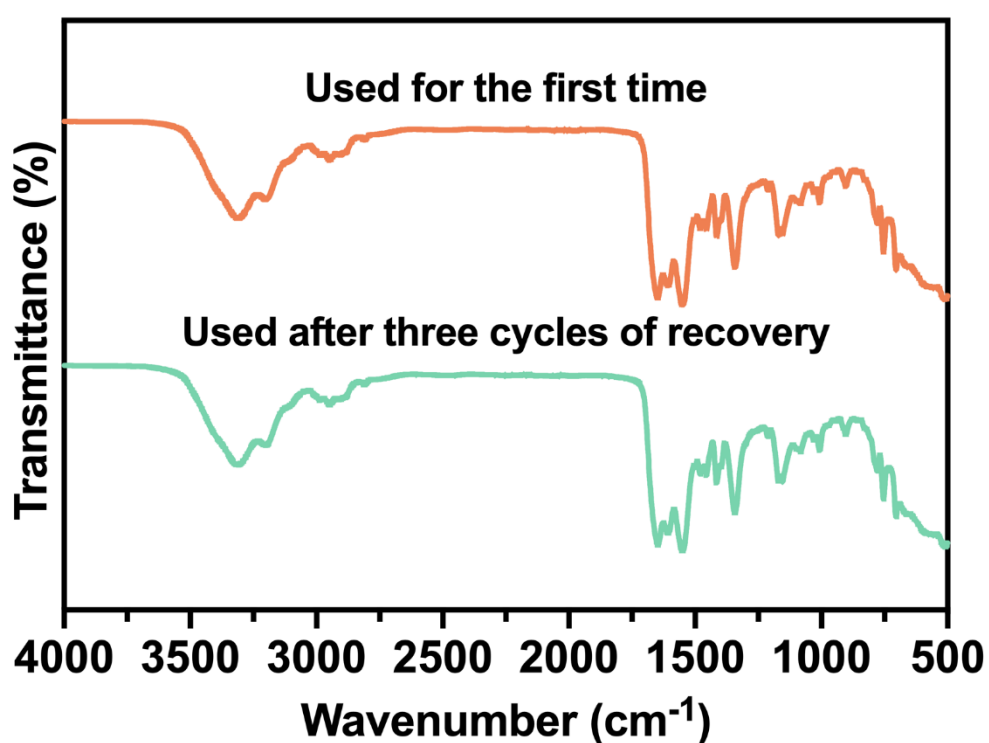


Fig. S5. FTIR spectra of DES before and after reuse.

Table S6. Mass balance and green metrics of the DES-based agarose extraction process

	Value	Notes	
	<i>Gelidium amansii</i>	3.00 g	dry weight
	DES	30.00 g	
Input	Ethanol	224.87 g	Used for precipitation: 177.53 g; used for washing: 47.34 g
	water	135.00 g	Used for dilution: 75 g; used for washing: 60 g
Output	Agarose	0.495 g	
	Solid residue	1.98 g	
	Recovered DES	21.42 g	
	Ethanol and water distillate	222.08 g	Ethanol concentration: 77.87%
	Recovered washing ethanol	47.34 g	
	Washing water	60.00 g	
	DES recovery yield	71.4%	
	Ethanol recovery yield	98.0%	
	Water footprint	0.273 m ³ ·kg ⁻¹	
	Energy consumption	6300 MJ·kg ⁻¹	Cumulative energy demand, calculated based on the heating process
	E-factor	30.6 kg·kg ⁻¹	Ratio of dry waste mass to product mass

Table S7. Mass balance and green metrics of the alkali-EDTA agarose extraction process

	Value	Notes	
	<i>Gelidium amansii</i>	10.00 g	
	NaOH	10.50 g	
	H ₂ SO ₄	0.119 g	
Input	Oxalic acid	0.096 g	
	EDTA-Na ₂	0.130 g	
	NaClO	0.060 g	
	Water	4707 g	
	Agarose	0.495 g	
output	Solid residue	15.905 g	
	Wastewater	4707 g	
	Water footprint	5.93 m ³ ·kg ⁻¹	
	Energy consumption	32652 MJ·kg ⁻¹	Cumulative energy demand, calculated based on the heating process
	E-factor	20.0 kg·kg ⁻¹	Ratio of dry waste mass to product mass

Table S8. Material requirements for agarose prepared via DES and Alkali-EDTA methods

	DES method (g/g agarose)	Alkali-EDTA method (g/g agarose)
<i>Gelidium amansii</i>	6.06	12.59
DES	60.6	—
NaOH	—	13.22
H ₂ SO ₄	—	0.15
Oxalic acid	—	0.12
EDTA-Na ₂	—	0.16
NaClO	—	0.08
EtOH	454.3	—
Water	273	5930

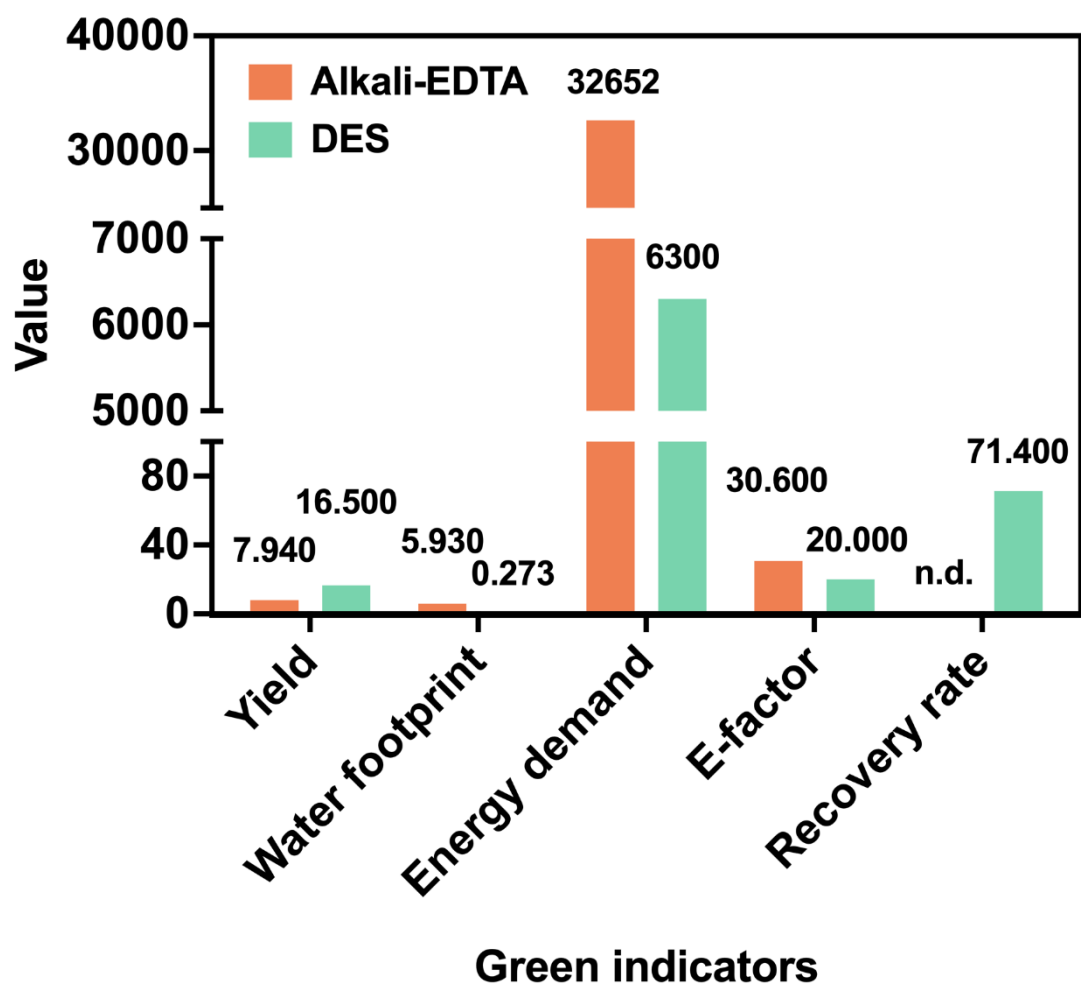


Fig. S6. Comparison of green indicators for DES and alkali-EDTA agarose extraction processes.